Structural and Electrical Properties of SnO_2:F Thin Films Prepared by Chemical Vapor Deposition Method

N. Najafi and S.M. Rozati
CVD Laboratory, Physics Department, University of Guilan, 41938-33697 Rasht, Iran

(Received August 10, 2015; in final form January 22, 2017)

Fluorine doped tin oxide (FTO) thin films were deposited onto glass substrate at different substrate temperatures by a simple and inexpensive method of air pressure chemical vapor deposition. The substrate temperature was kept constant at about 500 °C as the optimum temperature, and air was used as both a carrier gas and the oxidizing agent. A very simple method of characterization were carried on to investigate the electrical and structural properties of the prepared thin films. The electrical parameters variations showed that these parameters vary with substrate temperature ranging from an insulator thin film to a highly conductive layer. X-ray diffraction also revealed the structure to be polycrystalline at higher temperatures compared to amorphous structure for lower temperatures.

DOI: 10.12693/APhysPolA.131.222

PACS/topics: chemical vapor deposition, SnO_2:F thin films, structural properties, electrical properties

1. Introduction

The growing of optoelectronic applications such as solar cells, electrochromic devices or flat panels causes a demand for transparent conductive oxides (TCOs) [1–5]. Non-stoichiometric and doped films of oxides of cadmium, tin, zinc, indium, and their various alloys, which are deposited by various techniques, show high transmittance in the visible optical range, high reflectance in the IR region, and very high conductivity. Based on these fantastic properties, some of the TCOs applications include transparent electrodes in solar cells [6], light emitting diodes [7], liquid crystal displays [8], heat mirrors [9], dye-synthesized solar cells [10], wave guide electron devices [11], thick-film sensors [12], organic light emitting diodes [13], flat panel displays [14] and so on. TCOs are generally manufactured as undoped and doped form of indium oxide (In_2O_3), tin oxide (SnO_2), zinc oxide (ZnO) and cadmium oxide (CdO) which show high visible transmittance, high electrical conductivity, and high near IR reflectivity which is applicable in energy conserving [15]. Tin oxide thin films are well-known for their economical production and stability towards atmospheric conditions [16]. Traditionally, tin oxide is doped to improve its expected properties by some dopants such as indium [17, 18], antimony [19], palladium [20], cobalt [21] and fluorine. Depositing fluorine doped tin oxide thin films is usually done by spray pyrolysis [22], sputtering [23], sol-gel [24], and chemical vapor deposition (CVD), which in turn includes different variations such as low pressure CVD [25], plasma enhanced CVD [26], and atmospheric pressure chemical vapor deposition (AP-CVD) which is very productive and economic [27, 28].

2. Experimental techniques

The glass substrates were degreased using water and bleach, then rinsed in deionized water. These glasses are cleaned ultrasonically in an acetone/ethanol mixture, then rinsed again in deionized water. The cleaned glass substrates are then placed in a tubular furnace. To avoid the oxidation of the glass substrate surface during heating the substrate, nitrogen flow is used to clean the tubular furnace before introducing the source materials.

Deposition was carried out in a previously adapted home-made air pressure chemical vapor deposition by our colleagues in another work [29], schematically shown in Fig. 1. It contains a horizontal tubular furnace which has a diameter of 8 cm and about 100 cm long. The properties of films depend on various parameters such as ventilation flow rate, amount of evaporating precursors, deposition time and substrate temperature. The samples were grown at different substrate temperatures from 325 °C to 600 °C and constant $SnCl_2$ mass for 5 min.

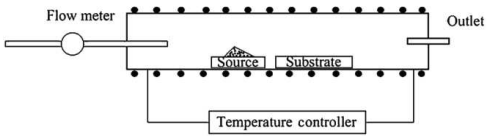

Fig. 1. Air pressure chemical vapor deposition [13].

0.1 g of $SnCl_2$ powder was added to different amounts of NaF (ranging 2–30 wt%) as the precursor. The layers structures were studied by X-ray diffraction (XRD) using an X-ray diffractometer with 1.54060 Å Cu K_α ray (PHILIPS PW 1840 apparatus). The optical properties are studied with a UV–visible spectrophotometer (Cary 100 Scan Varian) in the wavelength range of 250–800 mm at room temperature. We define the sheet resistance R_{sh} as follows: R_{sh} is related to the resistivity by

$$R_{sh} = \frac{\rho(t)}{t} = \frac{1}{\sigma(t)t}. \tag{2.1}$$

The dependence of σ on the film thickness t is implicit, through stoichiometric and microstructural changes with changes in film thickness. The average transmittance of an unsupported film at any wavelength is given by

$$T_\lambda = (1 - R_\lambda)^2 \exp(-\alpha_\lambda t), \tag{2.2}$$

where R_λ is the reflection coefficient and α_λ is the absorption coefficient which in the visible region is primarily due to free carriers [30].

TABLE I

Variations in the figure of merit with different temperatures T_s for $\lambda = 550$ nm

T_s [°C]	T [%]	R_{sh} [Ω/□]	$\Phi_M = T^{10}/R_{sh}$
325	88.18	34×10^6	0.9×10^{-9}
350	83.67	35×10^3	4.8×10^{-6}
450	64.81	97	1.35×10^{-4}
500	54.42	14	1.63×10^{-4}
600	65.18	62	2.23×10^{-4}

Haacke made a great contribution and defined a useful figure of merit,

$$\Phi_M = \frac{T^{10}}{R_{sh}}, \tag{2.3}$$

where T is the transmittance at $\lambda = 550$ nm and R_{sh} is the sheet resistance. Φ_M value was supposed to directly reflect the performance of the TCO applications [31] (Table I).

3. Results and discussions

The sheet resistance was found to decrease with increasing the substrate temperature to a minimum of 14 Ω/□ at $T_s = 500$ °C (Table I). Wang et al. minimum sheet resistance for FTO layers using APCVD is in the range of 8–11 Ω/□ [32]. The obtained R_{sh} values are less than a few reported for these films which are 38 Ω/□ [33, 34], 136 Ω/□ [35], and 30 Ω/□ [36]. Also, our work is considered unique in terms of the deposition timing, only 5 min. Shadia et al. explain that in the beginning the resistivity decreases due to the growth of grain size but when the crystal growth is complete no further increase in grain size occurs, from this point on, by increasing the substrate temperature, the removal of chlorine that was incorporated as $SnCl_2$ and improvement of stoichiometry results in an increase in the resistivity [37]. Tahi et al. also explain that the absorption of oxygen at the films surface and an increase in SiO_2 thickness at interface SnO_2/Si at very high temperatures causes the sheet resistance to increase [35]. The conductivity of non-stoichiometric tin oxide films is influenced by the presence of doubly ionized vacancies serving as donors. When fluorine is incorporated in tin oxide films, each F^- anion substitutes an O^{2-} anion in the lattice and the substituted O^{2-} anion introduces more free electrons. This is probably resulting in an increase in free electrons and decreases the value of R_{sh}. At higher doping concentrations the sheet resistance increases which is probably suggesting that the excess F atoms do not occupy the proper lattice positions, and at the same time may increase the structural disorder [16, 38]. Compared to other dopants such as antimony, the minimum sheet resistance of 8 Ω/□ for a 3% doping has achieved [19]. Antimonium tin oxide (ATO SnO_2:Sb) was also deposited using atomic layer epitaxy and the optimum resistivity of $\approx 10^{-3}$ Ωcm [39], comparable to our results which is 1.75×10^{-3} Ωcm (sheet resistance = 14Ω/□).

Figure 2 shows the X-ray diffraction patterns of SnO_2:F thin films deposited by the CVD technique at different substrate temperatures. When the substrate temperature during deposition is low (less than 350 °C), the resultant SnO_2:F films exhibit an amorphous structure. Increasing substrate temperature causes the FTO thin films to exhibit a strong orientation along (200). There is no feature of fluoride in the patterns of FTO films, providing the experimental evidence of the incorporation of fluorine into the SnO_2 lattice. The films deposited at about $T_s > 450$ °C present a polycrystalline structure. The narrowing of the lines of crystal growth at the higher substrate temperature means that the grain size had increased [37]. At temperatures higher than 500 °C, the crystalline changes because of the Si interference from the substrate into our thin film and we can see new orientations at 600 °C. Figure 3 shows the X-ray diffraction patterns of SnO_2:F thin films deposited by the CVD technique with different fluorine weight percents. Only with 5 wt% of the fluorine dopant, we could find the (200) orientation and as we move towards higher dopant concentrations, the film structure shows a more amorphous thin film.

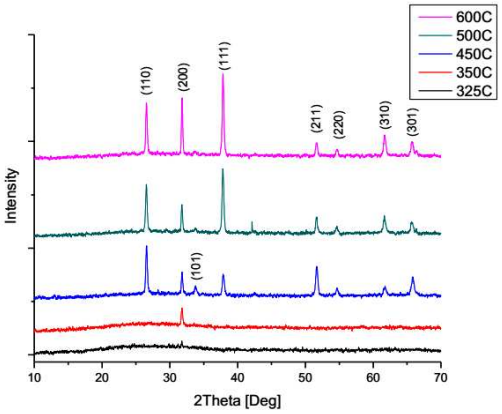

Fig. 2. X-ray diffraction spectra of SnO_2:F thin films at different substrate temperatures (325, 350, 450, 500, and 600 °C) for 5 min.

The values of thickness were determined using Eq. (3.1):

$$d = \lambda_1\lambda_2/2(\lambda_1 n(\lambda_2) - \lambda_2 n(\lambda_1)), \tag{3.1}$$

where $n(\lambda_1)$ and $n(\lambda_2)$ are the refractive indices corresponding to the wavelengths λ_1 and λ_2, respectively [40].

Based on the calculations, the amount of used precursor powder is almost in direct proportion with the film thickness as expected. The measured thickness for 0.1, 0.2, 0.3, 0.4, and 0.5 were 800, 1600, 2400, 3200, and 4000 nm, respectively. We considered 800 nm thickness produced using 0.1 g of the powder mixture as the best thickness for the rest of this work and kept it constant.

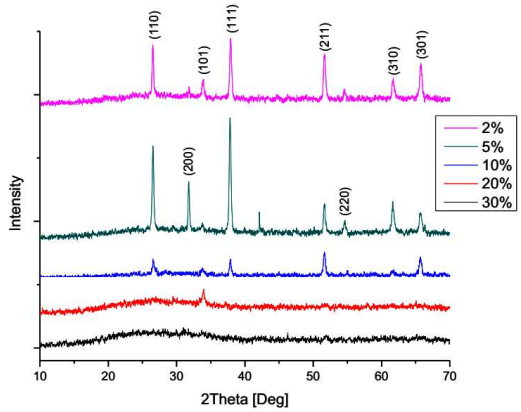

Fig. 3. X-ray diffraction spectra of SnO_2:F thin films with different fluorine wt% (2, 5, 10, 20, and 30) for 5 min.

By increasing the film thickness, we get a better sheet resistance but the transparency sacrificed (Fig. 2). Depending on the application, one may utilize a thicker layer with a one digit sheet resistance or a thin layer with high transparency. As an electrode, we may use a thick layer (> 2 μm) for higher conductivity and for higher transparency one may use thinner layers (< 1 μm). We considered $T_s = 500\,^{\circ}$C as the best substrate temperature for the rest of this work.

Figure 4 shows the transmittance and sheet resistance with different thin film thickness. By increasing the thickness, electrical resistance and transparency decrease. The transparency reduction could be attributed to the absorption via states within the gap [13]. Layers show bulk state properties in higher amounts of the powder mixture in a way that we see 54.42% and 16.5% transmittance ($\lambda = 550$ nm) for the thinnest and the thickest films, respectively. Therefore, the decreasing transmittance was mainly due to the increasing thickness of FTO films [41].

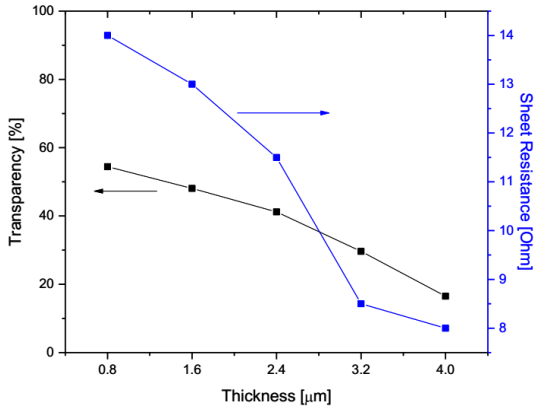

Fig. 4. Transparency and sheet resistance variations with different thin film thicknesses.

Figure 5 shows the optical transmittance of SnO_2:F thin films (800 nm thickness) with different substrate temperatures. Optical transmittance measurements of

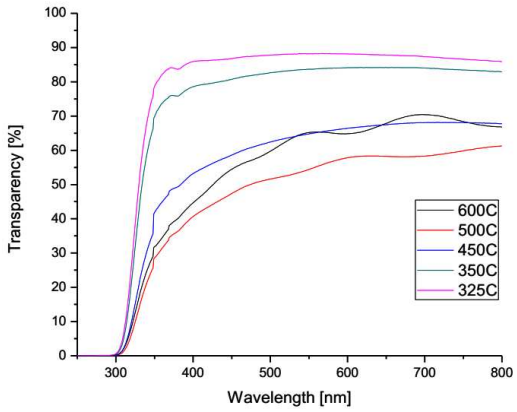

Fig. 5. Optical transmittance of SnO_2:F (800 nm thickness) thin films with different substrate temperatures (320, 350, 450, 500, and 600 °C).

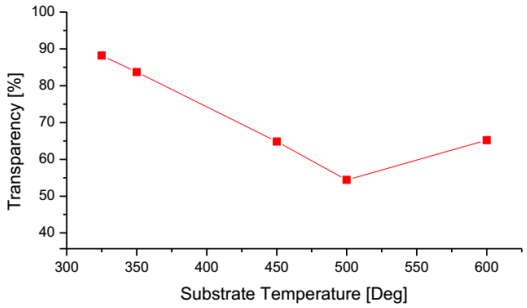

Fig. 6. Transparency vs. temperature of SnO_2:F (800 nm thickness) in $\lambda = 550$ nm.

SnO_2:F shows that in the temperature range of 325 °C to 600 °C, with increasing substrate temperature, transmittance decreases up to around 500 °C. This can be explained by carrier concentration increase and so increase of absorbance and transmission decrease. Also, it can be related to the polycrystalline structure of tin oxide film at temperatures up to 500 °C. As we increase the substrate temperature, transmittance improves and at 600 °C we reach to a maximum of 65.18% with all the other parameters kept constant. Fluorine doped tin-oxide was found to be governed by its free electron properties in the infrared while it exhibits the features of a wide band gap semiconductor in the UV and lower part of the visible [42]. Figure 6 shows the variations of transparency in different temperatures for a 800 nm thickness FTO film.

4. Conclusions

XRD measurements indicated that the SnO_2:F films were preferentially oriented along (200) for temperatures $T_s > 500\,^{\circ}$C, which means the crystal growth was enhanced and the grain size had increased. The best films sprayed at 500 °C with lowest sheet resistance 14 $\Omega/\square$. The maximum transparency of 88.18% (at wavelength of 550 nm) is observed when substrate temperature is kept at 325 °C. Our best sample was the one with 54.42% transparency and 14 $\Omega/\square$ of resistance, simultaneously. We can conclude that the substrate temperature is an

effective parameter on the properties of FTO thin layers. In this paper, thin films of fluorine doped tin oxide prepared on glass substrates by the simple technique of APCVD. The variation of sheet resistance, resistivity, carrier concentration and mobility with temperature were investigated. The results indicate that the best resistivity can be achieved at substrate temperature of 500 °C. XRD analysis revealed that SnO_2 deposited at 400 °C are mainly amorphous whereas films deposited at the substrate temperature of above 450 °C have fine polycrystalline with the tetragonal rutile structure. Investigation of temperature effects on optical transmittance also revealed a reduction of transmittance and bandgap with increasing temperature.

Acknowledgments

The authors gratefully acknowledge the research department of University of Guilan.

References

[1] I. Sorar, D. Saygin-Hinczewski, M. Hinczewski, F.Z. Tepehan, *Appl. Surf. Sci.* **257**, 7343 (2011).

[2] J.-S. Cho, Y.-J. Kim, J.C. Lee, S.-H. Park, K.H. Yoon, *Solar En. Mater. Solar Cells* **95**, 190 (2011).

[3] Z.A. Wang, J.B. Chu, H.B. Zhu, Z. Sun, Y.W. Chen, S.M. Huang, *Solid-State Electron.* **53**, 1149 (2009).

[4] Z. Tebby, O. Babot, D. Michau, L. Hirsch, L. Carlos, T. Toupance, *J. Photochem. Photobiol. A Chem.* **205**, 70 (2009).

[5] C.-Y. Tsay, H.-C. Cheng, Y.-T. Tung, W.-H. Tuan, C.-K. Lin, *Thin Solid Films* **517**, 1032 (2008).

[6] B. Liu, H.C. Zeng, *J. Phys. Chem. B* **108**, 5867 (2004).

[7] V. Palenskis, J. Matukas, S. Pralgauskaitė, *Solid-State Electron.* **54**, 781 (2010).

[8] N. Yamamoto, H. Makino, S. Osone, A. Ujihara, T. Ito, H. Hokari, T. Maruyama, T. Yamamoto, *Thin Solid Films* **520**, 4131 (2012).

[9] M.F. Al-Kuhaili, A.H. Al-Aswad, S.M.A. Durrani, I.A. Bakhtiari, *Solar En.* **83**, 1571 (2009).

[10] A.Y. El-Etre, S.M. Reda, *Appl. Surf. Sci.* **256**, 6601 (2010).

[11] Y. Chen, X. Cui, K. Zhang, D. Pan, S. Zhang, B. Wang, J.G. Hou, *Chem. Phys. Lett.* **369**, 16 (2003).

[12] G. Sberveglieri, C. Baratto, E. Comini, G. Faglia, M. Ferroni, A. Ponzoni, A. Vomiero, *Sens. Actuat. B Chem.* **121**, 208 (2007).

[13] D. Vaufrey, M.B. Khalifa, M.P. Besland, C. Sandu, M.G. Blanchin, V. Teodorescu, J.A. Roger, J. Tardy, *Synth. Met.* **127**, 207 (2002).

[14] J.L. Kwo, M. Yokoyama, W.C. Wang, F.Y. Chuang, I.N. Lin, *Diam. Relat. Mater.* **9**, 1270 (2000).

[15] M. Batzill, U. Diebold, *Prog. Surf. Sci.* **79**, 47 (2005).

[16] N. Memarian, S.M. Rozati, E. Elamurugu, E. Fortunato, *Phys. Status Solidi C* **7**, 2277 (2010).

[17] K.F. Toshiro Maruyama, *Thin Solid Films* **203**, 297 (1991).

[18] T. Maruyama, K. Fukui, *J. Appl. Phys.* **70**, 3848 (1991).

[19] S. Haireche, A. Boumeddiene, A. Guittoum, A. El Hdiy, A. Boufelfel, *Mater. Chem. Phys.* **139**, 871 (2013).

[20] H.-K. Seo, S.G. Ansari, S.S. Al-Deyab, Z.A. Ansari, *Sens. Actuat. B Chem.* **168**, 149 (2012).

[21] A.M. El Sayed, S. Taha, M. Shaban, G. Said, *Superlatt. Microstruct.* **95**, 1 (2016).

[22] Y.T.B. Zhang, J.X. Zhang, W. Cai, *J. Optoelectron. Adv. Mater.* **13**, 89 (2011).

[23] Z. Banyamin, P. Kelly, G. West, J. Boardman, *Coatings* **4**, 732 (2014).

[24] S. Wu, S. Yuan, L. Shi, Y. Zhao, J. Fang, *J. Coll. Interf. Sci.* **346**, 12 (2010).

[25] A. Chowdhury, D.-W. Kang, M. Isshiki, T. Oyama, H. Odaka, P. Sichanugrist, M. Konagai, *Solar En. Mater. Solar Cells* **140**, 126 (2015).

[26] M. Jubault, J. Pulpytel, H. Cachet, L. Boufendi, F. Arefi-Khonsari, *Plasma Proc. Polym.* **4**, S330 (2007).

[27] J.T. Wang, X.L. Shi, X.H. Zhong, J.N. Wang, L. Pyrah, K.D. Sanderson, P.M. Ramsey, M. Hirata, K. Tsuri, *Solar En. Mater. Solar Cells* **132**, 578 (2015).

[28] J. Yang, W. Liu, L. Dong, Y. Li, C. Li, H. Zhao, *Appl. Surf. Sci.* **257**, 10499 (2011).

[29] M. Maleki, S.M. Rozati, *Bull. Mater. Sci.* **36**, 217 (2013).

[30] K.L. Chopra, S. Major, D.K. Pandya, *Thin Solid Films* **102**, 1 (1983).

[31] G. Haacke, *J. Appl. Phys.* **47**, 4086 (1976).

[32] Y. Wang, Y. Wu, Y. Qin, Z. Zhang, C. Shi, Q. Zhang, C. Li, X. Xia, S. Sun, L. Chen, *Mater. Res. Bull.* **46**, 1262 (2011).

[33] A.M. Jafar, K. Al-Amara, F.L. Rashid, I.K. Fayyadh, *Int. J. Innovat. Res. Eng. Sci.* **6**, 49 (2013).

[34] K.C. Molloy, J.E. Stanley, *Appl. Organomet. Chem.* **23**, 62 (2009).

[35] M.B.H. Tahi, R. Talaighil, M.S. Belkaid, M. Goudjil, *Afric. Phys. Rev.* **2**, 89 (2008).

[36] H.-L. Zhao, Q.-Y. Liu, Y.-X. Cai, F.-C. Zhang, *Am. Ceram. Soc. Bull.* **86**, 9201 (2007).

[37] S.J. Ikhmayies, R.N. Ahmad-Bitar, *Mater. Sci. Semicond. Process.* **12**, 122 (2009).

[38] K.R.E. Elangovan, *J. Optoelectron. Adv. Mater.* **5**, 45 (2003).

[39] H. Viirola, L. Niinistö, *Thin Solid Films* **251**, 127 (1994).

[40] S. Ilican, M. Caglar, Y. Caglar, *Mater. Sci. Poland* **25**, 709 (2007).

[41] X. Huang, Z. Yu, S. Huang, Q. Zhang, D. Li, Y. Luo, Q. Meng, *Mater. Lett.* **64**, 1701 (2010).

[42] K.V. Rottkay, M. Rubin, *Mater. Res. Soc. Symp. Proc.* **426**, 449 (1996).